Thermochimica Acta, 80 (1984) 149–163
Elsevier Science Publishers B.V., Amsterdam – Printed in The Netherlands

THE THERMAL DECOMPOSITION OF SOME PRIMARY EXPLOSIVES AS STUDIED BY DIFFERENTIAL SCANNING CALORIMETRY

D.J. WHELAN, R.J. SPEAR and R.W. READ

Physical Chemistry Division, Materials Research Laboratories, Department of Defence, Commonwealth of Australia, P.O. Box 50, Ascot Vale, Victoria (Australia)

(Received 23 April 1984)

ABSTRACT

Most currently used stab- and percussion-sensitive mixes consist of lead azide, lead styphnate or lead dinitroresorcinate in admixture with 2–5% tetrazene, which functions as an energetic sensitizer. A major problem with the use of such compositions is the poor thermal stability of tetrazene, depletion of which leads to loss of activity. The thermal decomposition of some 24 compounds, all identified as potential replacements for tetrazene in stab and percussion mixes, has been studied by non-isothermal differential scanning calorimetry, and the physicochemical parameters which characterise these explosive reactions have been determined and compared with data from temperature of ignition measurements.

INTRODUCTION

Most currently used stab- and percussion-sensitive mixes consist of a primary explosive lead salt, usually the azide, styphnate or dinitroresorcinate, in admixture with 2–5% of the primary explosive, tetrazene, and other components. The high sensitivity of these compositions is due primarily to tetrazene (**1**) which functions as an "energetic sensitizer". However, a major drawback to the use of such compositions is the poor thermal stability of tetrazene, deterioration of which may result in failure of the composition in service, and "dudding" of the device. There is, consequently, considerable interest in finding new primary explosives which possess a sensitizing ability comparable to that of tetrazene but with enhanced thermal stability.

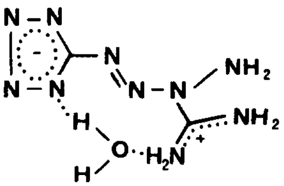

TETRAZENE

A research programme has been undertaken in these Laboratories to prepare and investigate new materials of this type, and several very promising compounds have been prepared [1–3]. The subject of this report is the investigation of the thermal characteristics of some of these materials.

Stab-initiation occurs by penetration of the compacted explosive increment by a fast-moving needle or firing pin. Experimental evidence is consistent with the notion that the initiation process is thermal in origin [1,4,5]; either friction between the impacting needle and hard crystalline particles [5a] (for example lead azide or added gritty materials) or friction between adjacent crystals [5b] generates local "hot spots". In a mixture containing tetrazene, tetrazene particles in the immediate vicinity of the "hot spot" ignite when the ignition temperature, T_I, is exceeded (136 °C, 409 K), additional heat is thus generated and this ignites the lead azide ($T_I = 316$ °C, 589 K) which detonates.

The strong sensitizing ability of tetrazene has been attributed primarily to its low T_I [6], although a more detailed investigation has found that there is only a general trend to increased sensitization with decreasing T_I [1].

T_I is determined by a rather simple, "traditional" test: 50 mg of the material are heated at a rate of 5 K min^{-1} until ignition (usually explosion) occurs, the temperature at which this occurs being defined as T_I. On the other hand, differential scanning calorimetry (DSC) is a much more sensitive probe with which not only the ignition characteristics but also kinetic parameters, such as activation energies, can be determined and ignition mechanisms investigated.

In this paper, the authors report on the thermal behaviour of 24 primary explosives, as studied by DSC, and compare the information obtained with experimentally-determined T_I values.

EXPERIMENTAL

Materials

The following compounds have been studied: tetrazene (**1**); various 6-azido-2,4-dinitrophenolates, namely Ag(I), Pb(II), Na, K and Ba (**2**–**6**); 5-nitro-2-picryl-tetrazole (**7**); mercuric and mercurous bis(5-nitrotetrazolate) (**8**,**9**); mercuric bisfulminate (**10**); 6-diazo-2,4-dinitrophenolate (**11**); 3-methyl-6-diazo-2,4-dinitrophenolate (**12**); silver(I) 5-nitrotetrazolate (**13**); dithallous 5,5′-azobis(tetrazolate) (**14**); dilead(II) 5,5′-azobis(tetrazolate) dihydroxide (**15**); 5,5′-hydrazobis(1*H*-tetrazole) (**16**); lead (II) azide (**17**); and a family of compounds derived from 4,6-dinitrobenzofurazan 1-oxide, namely: potassium 4-hydroxy-5,7-dinitro-4,5-dihydrobenzofurazanide 3-oxide (**18**) (commonly known in explosives literature as KDNBF, potassium dinitrobenzofuroxan); potassium 4-methoxy-5,7-dinitro-4,5-dihydrobenzofur-

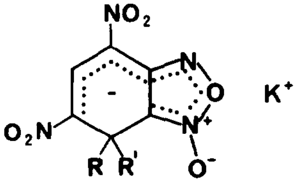

R	R'	
OH	H	(18)
OMe	H	(19)
NHOH	H	(20)
=N—OH		(21)

azanide 3-oxide (**19**); potassium 4-hydroxyamino-5,7-dinitro-4,5-dihydrobenzofurazanide 3-oxide (**20**); potassium 4-hydroxyamino-5,7-dinitrobenzofurazanide 3-oxide (**21**); 4-(4′-ammoniophenyl)-5,7-dinitro-4,5-dihydro-

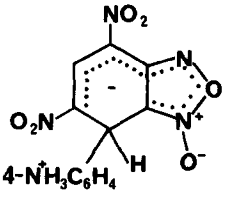

(22)

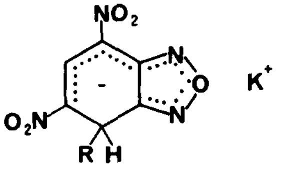

R	
OH	(23)
OMe	(24)

benzofurazanide 3-oxide (**22**); potassium 4-hydroxy-5,7-dinitro-4,5-dihydrobenzofurazanide (**23**); and potassium 4-methoxy-5,7-dinitro-4,5-dihydrobenzofurazanide (**24**).

The structures of compounds **2**–**17** are given in ref. 1; the structures of compounds **18**–**24** are given within this text.

Tetrazene (type RD1357) was available from a sample prepared at Materials Research Laboratories for other studies. Ignition temperature 136 (2 ×) °C, 137 °C.

Lead azide (type RD1343) was obtained as a single batch from Munitions Filling Factory, St. Marys, NSW. Ignition temperature 315 °C, 316(2 ×) °C (lit. 320 °C [1]).

The preparation of the remaining compounds has been described fully in publications from these Laboratories. The preparation has been previously

TABLE 1

Ignition temperatures and thermal analytical data for compounds **1–16**

Compound	T_I		DSC characteristics			Thermogram appearance
	°C	K	T_m (5 K min^{-1}) (K)	E^* (kJ mol^{-1})	$\log_{10} A$ (s^{-1})	
1	136	409	410.8	163	18.7	Ignition exotherm then broader secondary exotherm (see [13])
2	122	395	399.9	120	13.6	Single exotherm
3	126	399	382.4	84	21.4	Smaller exotherm followed by much larger exotherm [a]
			403.2	180	9.2	
4	131	404	411.0	120	13.1	Series of small, broad exotherms, then large exotherm
5	133	406	405.9	119	13.1	Single exotherm
6	159	432	431.6	152	16.5	Single exotherm
7	156	429	438.7	269	30.2	Single exotherm (see Fig. 1)
8	206	479	505.2	157	14.0	Single exotherm
9	205	478	465.0	114	10.5	Smaller exotherm followed by overlapping larger exotherm [a]
			493.5	189	17.9	
10	158	431	447.2	117	11.5	Broader first exotherm overlapping sharper exotherm (see Fig. 2)
11	160	433	440.0	178	42.5	Endotherm (melting) underlying exotherm (see Fig. 3)
12	178	451	457.6	174	17.9	Single exotherm
13	261	534	554.8	176	14.3	Broad exotherm with underlying endotherm
14	212	485	479.6	183	17.8	Single exotherm
15	230	503	503.9	184	17.0	Single exotherm
16	229	502	511.0	251	23.7	Sharp exotherm with underlying endotherm
17	316	589	586.1	197	15.3	First exotherm followed by smaller secondary exotherm

[a] The top line refers to the first exotherm, the data below to the second exotherm.

TABLE 2

Ignition temperatures and thermal analytical data for compounds **18**–**24** derived from 4,6-dinitrobenzofurazan 1-oxide

Compound	T_I		DSC characteristics			Thermogram appearance
	°C	K	T_m (5 K min^{-1}) (K)	E^* (kJ mol^{-1})	$\log_{10} A$ (s^{-1})	
18	200	473	489.4	179	17.0	Large first exotherm [a] followed by broad secondary exotherm
19	181	454	455 467 476	133 114 101	13.0 10.5 8.8	Three successive exotherms of approximately equal intensity; data are given for all three
20 Maroon form	135	408	404 421	127 184	14.3 21.0	Small initial exotherm followed by much larger second exotherm, then a third weaker shoulder [b]
Brick red form	143	416	431 436	175 164	18.2 17.6	Two very closely spaced exotherms of comparable intensity
Chocolate form	144	417	424	188	21	Intense exotherm [a] with poorly resolved shoulders either side
21	140	413	431	229	25.8	Sharp first exotherm [a] followed by a series of small exotherms
22	217	490 [c]	478	146	13.8	First intense exotherm [a] with following shoulder
23	223	496	496.5	228	21.9	Intense exotherm [a] followed by smaller broader secondary exotherm
24	180	453	466	243	25.4	Intense exotherm [a] possibly with underlying initial exotherm, then two weak secondary exotherms

[a] Data given only for this peak.

[b] No data given for this peak.

[c] Burnt with a fizz, no explosion.

described for compounds **2–16** and **18** [1], **19** [7], **20** [3], **22** [9], **23** and **24** [10], and the preparation of compound **21** is to be published [8].

The ignition temperatures of these compounds and the kinetic characteristics of their thermal decompositions, as determined by non-isothermal differential scanning calorimetry, are summarized in Tables 1 (compounds **1–17**) and 2 (compounds **18–24**).

METHODS

Temperature of ignition

Ignition temperatures were determined on an instrument built to specifications for the ERDE temperature of ignition test *. As mentioned in the Introduction, unconfined 50-mg samples were heated at 5 °C min^{-1} in a test tube, the temperature of ignition being that temperature at which the samples ignited to explosion or fast burn. These tests were carried out by the Explosives Testing Group, MRL, under the direction of Mr. D.J. Pinson.

Differential scanning calorimetry

Thermochemical measurements were obtained using a Perkin-Elmer DSC-2 differential scanning calorimeter fitted with a Scanning Auto-Zero (SAZ) accessory. All samples were accurately weighed on a Mettler ME30 analytical balance, directly into aluminium sample pans, and lids placed (but not crimped) over the samples. The sample mass in most cases was 0.20 ± 0.02 mg.

The sample and reference compartments of the calorimeter were continuously purged with nitrogen gas throughout the DSC scans, which were carried out at heating rates from 2.5 to 40 K min^{-1} over a temperature range usually from 340 to 600 K and above. The nitrogen flow rate was typically 20–25 ml min^{-1}.

The output of the DSC-2 differential scanning calorimeter was calibrated using samples of indium (m.p. 429.7 K) and tin (m.p. 505.1 K).

In many cases, it was necessary to operate the differential scanning calorimeter in a high sensitivity mode (for example, range 2 mcal s^{-1} full scale 10 mV deflection, or less) using a "minimum weight" of sample (ca. 0.20 mg) rather than increase the weight of sample and operate at a lower sensitivity. This was done both to standardize reaction conditions and to ensure that the DSC traces represented thermal changes arising from reac-

---

* Explosives Research and Development Establishment, Waltham Abbey, Essex, U.K. In 1977, it underwent a name change and is now known as PERME (Propellants, Explosives and Rocket Motor Establishment).

tions in thermal equilibrium with their surroundings. When larger masses of sample were used, particularly for those compounds with relatively low ignition temperatures ($\lesssim 180\,^{\circ}$C, 453 K), thermal decomposition often occurred rapidly, a large output of heat being generated very quickly with loss of thermal equilibrium, and the DSC "peak" often ran "off scale". This probably corresponded to "ignition" followed by "thermal explosion"; in most of these cases, the sample lid was blown off the pan in the DSC sample compartment.

Kinetic parameters from DSC data

The kinetic parameters of thermal decomposition, namely, E^*, the activation energy, and the apparent first-order Arrhenius pre-exponential term, A, were determined from Kissinger's treatment of DSC data [11], as described by Patel and Chaudhri [12].

It has been found that the peak temperature, or temperature at which the rate of dissipation of heat from an exothermic reaction is greatest, is a function of the rate of heating of the sample and a relationship exists between peak temperature and heating rate for a (pseudo) first-order reaction. This relationship can be summarized by the equation

$$A\ \exp(-E^*/RT) = \frac{E^*}{RT_{\mathrm{m}}^2}\frac{\mathrm{d}T}{\mathrm{d}t} \tag{1}$$

where R is the gas constant, T_{m} is the peak temperature and $\mathrm{d}T/\mathrm{d}t$ is the time rate of heating of the sample. This can be written as

$$\ln\left(\frac{\phi}{T_{\mathrm{m}}^2}\right) = \ln\left(\frac{R}{E^*}A\right) - \frac{E^*}{R}\frac{1}{T_{\mathrm{m}}} \tag{2}$$

where $\phi = \mathrm{d}T/\mathrm{d}t$, from which a plot of $\ln(\phi/T_{\mathrm{m}}^2)$ vs. $1/T_{\mathrm{m}}$ is a straight line, of slope $-E^*/R$.

Kissinger extended this approach to show that, even for an nth-order reaction, reasonable approximations can be made which reduce the kinetics to a form where this equation can apply, regardless of reaction order; the pre-exponential term, A^*, has the dimensions $(\text{time})^{-1}$ and can be regarded as a pseudo first-order constant.

It has been found that, in all the cases reported here, a plot of $\ln(\phi/T_{\mathrm{m}}^2)$ vs. $1/T_{\mathrm{m}}$ is generally linear, provided that only small masses are used and that the reaction is permitted to proceed under conditions where thermal equilibrium is maintained at all times; viz. heating rates, ϕ, not greater than 40 K min^{-1}.

The activation energies listed in Tables 1 and 2 were all obtained in this manner.

Rearranging eqn. (2) gives

$$\ln A = \ln\left(\frac{\phi}{T_m^2}\right) + \ln\left(\frac{E^*}{R}\right) + \frac{E^*}{R}\frac{1}{T_m} \quad (3)$$

which was evaluated for given ϕ and T_m values from the Kissinger plot for each compound, whereupon

$$\log_{10} A\ (\mathrm{s}^{-1}) = \frac{1}{2.30258}\left[\ln A\ (\mathrm{min}^{-1}) - \ln 60\right] \quad (4)$$

A typical Kissinger plot can be made from the data presented in Table 3 for 5-nitro-2-picryltetrazole (7). It was estimated that the magnitude of the errors in T_m would be ca. ±0.7 K, which would lead to an uncertainty in E^* of ca. ±5% and in $\log_{10} A$ (s^{-1}) of ca. ±3%. Uncertainties of this magnitude apply to all of the parameters determined from DSC data listed in Tables 1 and 2.

DSC traces

Representative traces from the recorder attached to the DSC apparatus were digitized and redrawn using a California Computer Products CALCOMP 600 series digitizer, employing software prepared by Mr R.P. Parker of these Laboratories, so as to present suitably scaled diagrams for discussion purposes.

These standard patterns (presented in Figs. 1–3) were typical of the DSC output of the various compounds studied here.

Pattern A

The DSC trace for compound 7 is shown in Fig. 1. This is an ideal reaction to study by Kissinger's method as it consists of only a single exotherm, corresponding to ignition. About one-half of the compounds listed in Table 1 exhibit this behaviour (see Notes, Table 1).

More often than not, however, the DSC traces are more complicated and several different patterns of behaviour can be identified.

TABLE 3

The effect of heating rate on peak temperature for thermal decomposition of 5-nitro-2-picryltetrazole (7)

Heating rate, ϕ (K min^{-1})	Peak temperature, T_m (K)
40	450.8
20	446.6
10	442.9
5	438.7
2.5	434.2

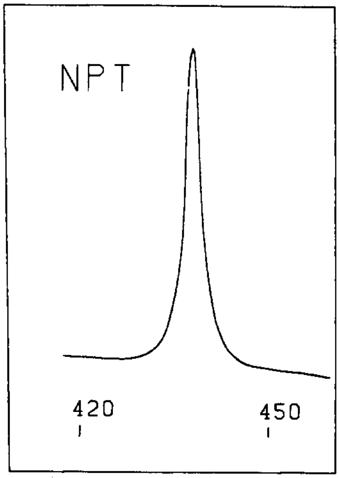

Fig. 1. DSC trace of 5-nitro-2-picryl-tetrazole (**7**) under dry nitrogen (flow rate 20–25 ml min^{-1}), heating rate 5 K min^{-1}. The abscissa is the temperature axis (K), the ordinate is in arbitrary units of $\mathrm{d}Q/\mathrm{d}T$, the rate of liberation of heat with temperature. The upward deflection of the curve peak denotes an exothermic reaction.

Pattern B

Some compounds have DSC traces displaying an intense ignition exotherm followed by one or more broader exotherms corresponding to secondary decomposition of the ignition products. These patterns are displayed by tetrazene (**1**) and several of the compounds listed in Table 2; most of the DSC "peaks" from this group of compounds lend themselves readily to analysis by the Kissinger method. This thermal behaviour of tetrazene has been described in quantitative detail by Patel and Chaudhri [12] and in qualitative terms by Norwitz et al. [13].

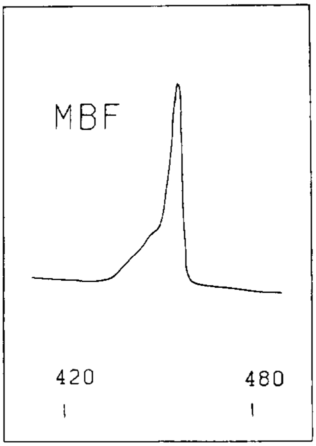

Fig. 2. DSC trace of mercuric bisfulminate (**10**) under dry nitrogen (flow rate 20–25 ml min^{-1}), heating rate 10 K min^{-1}.

Pattern C

A number of compounds exhibit two distinct exotherms where the first exotherm is generally "weaker" in intensity than the second and is often overlapped by it. This occurs in particular with compounds **3**, **9** and **10**, the DSC trace for **10** being given in Fig. 2.

Sometimes even more complicated traces are observed, suggesting that thermal decomposition is proceeding by a multiple-step process. This is the behaviour observed for most of the compounds listed in Table 2 and, where overlap of peaks occurs, it is not always possible to carry out a meaningful Kissinger assignment for all steps in the sequence of events accompanying the thermal decomposition.

Pattern D

Occasionally, exothermic decomposition of a compound is accompanied by or just preceded by melting (microscopy). This occurs with compound **11** whose DSC trace is given in Fig. 3.

Further examples are described in Table 1.

Here, application of the Kissinger method is on less reliable ground as the DSC trace is complicated by overlap of the exothermic component and the endothermic component, making assignment of the DSC "peaks" or "T_m" less meaningful. Nevertheless, the authors were able to estimate reasonable T_m values in many cases and obtained satisfactory straight-line plots using eqn. (2) for the various compounds listed in Tables 1 and 2.

Alternative treatments of DSC data

Kissinger's method is not the only approach that has been used to calculate the kinetic parameters, E^* and $\log_{10}A$, from DSC data obtained

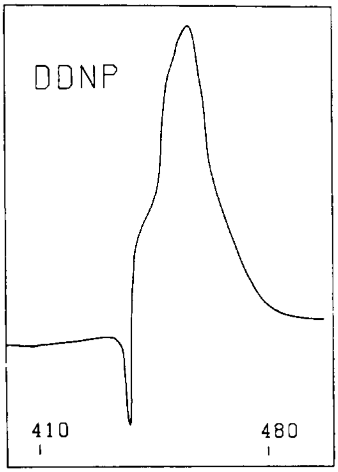

Fig. 3. DSC trace of 6-diazo-2,4-dinitrophenolate (**11**) under dry nitrogen (flow rate 20–25 ml min^{-1}), heating rate 20 K min^{-1}.

from solid-state reactions. However, it is the one which the authors have found to give consistent results with the compounds studied in Tables 1 and 2 and with other DSC studies.

Similar results have been obtained using Ozawa's method to determine E^*, the activation energy [14]. In this method

$$\log_{10}(\phi) + 0.4567\frac{E^*}{RT_m} = \text{a constant} \qquad (5)$$

For compounds **1–24**, it was found that a plot of $\log_{10}(\phi)$ vs. $1/T_m$ was very nearly linear and the activation energy was very similar to that obtained by Kissinger's method. This result was expected because the two equations (2 and 5) are very similar at high temperatures.

An alternative approach has been adopted by Rogers et al. [15]. They used data from a single non-isothermal DSC scan to obtain values of E^*. They assumed that, for a fixed mass of sample, the rate of evolution of heat is proportional to the reaction rate. However, the authors of this paper have found that the activation energies calculated by this method are much larger (factor of 3 or more, typically) than those calculated by Kissinger's method, the "fit" of the experimental data to the working equations is not always good, and the results are much less reproducible, run by run, at different heating rates. Part of the problem for this may reside in the fact that where overlapping exothermic reactions occur during thermal decomposition, as happens in many of the compounds under investigation here, the DSC traces were too complicated to analyse by Rogers' method.

As the aim of this paper has been to look for relative trends in reactivity and thermal sensitivity, the authors decided to do their comparisons from data calculated by Kissinger's method using the standardized weight of sample mentioned earlier. They assume that the relative figures have some meaning, although they accept the absolute figures may not be beyond dispute [16].

Where several exothermic reactions were observed to be occurring, the data contained in Tables 1 and 2 refer to the principal "low-temperature" decomposition reactions, i.e., the reactions which will lead to thermal decomposition.

DISCUSSION

The results for T_I and T_m in Tables 1 and 2 typically show that $T_m > T_I$.

In the DSC experiment, the "peak temperature", T_m, at a specified heating rate (5 K min^{-1} for direct comparison with T_I) corresponds to the maximum rate of transfer of thermal energy between the compound and its surroundings in the DSC apparatus. In contrast, T_I is determined on a much larger mass where no attempt is made to maintain thermal equilibrium, a situation conducive to "runaway" thermal decomposition. Indeed, most of the compounds examined in Tables 1 and 2 explode in the temperature of ignition test and the general trend of $T_m \geqslant T_I$ is thus expected.

In a number of cases, for example, for compounds **8**, **9** and **13**, the value of T_m is much greater than that of T_I. All of these compounds have DSC traces characterised by broad exotherms where the rate of release of heat at T_m is not very much greater than that observed several degrees above or below T_m. Clearly, if thermal equilibrium is not maintained in these cases, runaway ignition can occur at a temperature significantly below T_m, at an equivalent heating rate.

As mentioned earlier, the DSC traces for several compounds in Tables 1 and 2, including compounds **3**, **9** and **10**, exhibit at least two exotherms, the first (lower-temperature) exotherm often being "weaker" than the subsequent main exotherm.

Comparison of T_m and T_I for compounds **3** and **9** leads to the conclusion that it is the second, more intense "peak" which corresponds to ignition. In the case of compound **10**, it is not possible to identify which of the overlapping exotherms (Fig. 2) corresponds to the ignition reaction. Nevertheless, one can deduce from the DSC traces that these materials and compounds **20** and **24** decompose in a stepwise manner involving a pre-ignition reaction. This should have important ramifications for long-term stability considerations in that slow exothermic decomposition can be seen to be occurring well below either T_I or T_m.

The Arrhenius parameters, E^* and $\log_{10} A$, calculated from the Kissinger plots are also listed for compounds **1–24** in Tables 1 and 2 and it is reasonable to ask how these values compare with those from other investigations.

Unfortunately, there do not appear to be many studies other than those based on differential scanning calorimetry or differential thermal analysis so that a broadly-based comparison of data cannot be made. However, a selection of data available in the literature is presented in Table 4 and the results contained therein indicate that there is reasonable consistency between the results obtained from different laboratories and, when available, from different techniques [17–25].

The main limitation in these studies is that the products of thermal decomposition need to be established to ensure that comparison of the reported data is really justified. The complexities of this approach have been addressed by Brown and Swallowe [17] in their comprehensive study of the thermal decomposition of silver 5-nitrotetrazolate (**13**), mercuric bis(5-nitrotetrazolate) (**8**), and mercuric bisfulminate (**10**). These authors recognised that several steps are involved in the thermal decomposition of these compounds and that each step is described by its own set of kinetic parameters.

The activation energies, E^*, generally increase with increased T_m; how-

TABLE 4

Published kinetic parameters for compounds studied in this report

Compound	Method	Kinetic parameters		Ref.
		E^* (kJ mol^{-1})	$\log_{10} A$ (s^{-1})	
10	Gas evolution	130–135	—	4b, 18
	Mass loss	136	14.9	17
		106		19
8	Mass loss	(i) 160	15.3	17
	(2 stages)	(ii) 137	12.8	
	DSC	114	—	20
13	Mass loss	(i) 190	19.1	17
	(3 stages)	(ii) 240	22.5	
		(iii) 160	14.7	
1	DSC	193 ± 6	22.6	13
17	Gas evolution	123		22
(α-orthorhombic)	Manometric	160		23
		159		4b, p. 152
17 (β-monoclinic)	DSC	168	12.98	24
17 (RD1333)	DTA	181	14.4	25

ever, a number of exceptions are apparent. Compounds **7** and **16** in Table 1 and compounds **21**, **23** and **24** in Table 2 have unexpectedly high E^* and $\log_{10} A$ values. This is particularly true for compounds **7** and **16** and it is interesting to note that these are the only two covalent compounds in the whole set; compounds **1** and **22** are zwitterions and the remaining compounds are metal salts. Compounds **21**, **23** and **24** are very similar structurally to the other materials in Table 2 and again there is no apparent reason why such high E^* values are obtained for these particular compounds.

Compound **10** is interesting: the value of E^* from non-isothermal DSC (117 kJ mol^{-1}) is very low compared to that determined from mass loss and from gas-evolution techniques (130–136 kJ mol^{-1}; Table 4). The most likely explanation is that, in the temperature range between $T_\mathrm{I} = 431$ K, and $T_\mathrm{m} = 447$ K, the high temperature exotherm from which this activation energy was determined arises not from the primary decomposition but from a faster secondary decomposition. Unfortunately, the first exotherm (Fig. 2) is not resolved sufficiently for a determination of E^* by the Kissinger method.

How realistic are these values of E^* and $\log_{10} A$ in giving an indication of the thermal stability of the compounds in Tables 1 and 2?

Recently at MRL, Elischer and Spear [26] investigated the thermal stability of tetrazene (**1**) stored in an oven at 89 °C, in air. They found that tetrazene, as expected, decomposes relatively rapidly. Approximately 50% of tetrazene (small batch, well spread out) decomposed in ca. 28 days. In contrast, one may have predicted a half-life of ca. 13 h for tetrazene at 89 °C, using the parameters of Table 1 in the Arrhenius equation

$$k^1 = A\ \exp(-E^*/RT) \qquad (6)$$

One can also look at the thermal decomposition of lead(II) 6-azido-2,4-dinitrophenolate (**11**). Using the data from Table 1, one would expect that at 300 K (27 °C), this material would have a half-life of ca. 1×10^{-7} s; however, this compound appears stable at room temperature for an indefinite period. These examples highlight the problems associated with the extrapolation of data obtained from non-isothermal DSC methods (under idealized conditions) to predicting the service-life of potentially unstable compounds in practical environments. The mode of decomposition under two different sets of conditions is probably different.

CONCLUSION

The analysis of the DSC data presented herein relates to the pseudo first-order thermal decomposition reactions taking place in a series of explosive compounds, near their ignition temperatures, in an inert atmosphere and at atmospheric pressure. As such the data are useful for comparative purposes, since, in any explosive decomposition, the rate of release of energy is as important as the net amount of energy released. However, the reaction pathways accompanying the thermal decomposition of explosives under these conditions need not parallel those found during thermal decomposition at much lower temperatures. This can be seen by comparing the behaviour of tetrazene (**1**) and lead (II) 6-azido-2,4-dinitrophenolate (**11**), cited above, under reaction conditions which approximate to thermal ageing and to thermal explosion.

REFERENCES

1 R.J. Spear and P.P. Elischer, Aust. J. Chem., 35 (1982) 1.

2 R.J. Spear and P.P. Elischer, Materials Research Laboratories Report, 1982, MRL-R-859.

3 W.P. Norris and R.J. Spear, Materials Research Laboratories Report, 1983, MRL-R-870.

4 (a) F.P. Bowden and A.D. Yoffe, Initiation and Growth of Explosion in Liquids and Solids, Cambridge University Press, Cambridge, 1952, Chaps. 2, 3, 4.
(b) F.P. Bowden and A.D. Yoffe, Fast Reactions in Solids, Butterworth Scientific Publications, London, 1958, see in particular Chap. 5.

5 (a) M.M. Chaudhri, J.E. Field, J.T. Hagan and M. Coley, in P.J. Rolls (Ed.), Proc. 11th Congr. High Speed Photography, Chapman and Hall, London, 1974, p. 448.
(b) M.M. Chaudhri, Nature (London), 263 (1976) 121.

6 R. Bird, Materials Research Laboratories Report, 1975, MRL-R-362.

7 W.P. Norris, R.J. Spear and R.W. Read, Aust. J. Chem., 36 (1983) 297.

8 R.J. Spear and W.P. Norris, Materials Research Laboratories Report, 1984, in preparation.
9 R.J. Spear, W.P. Norris and R.W. Read, Tetrahedron Lett., 24 (1983) 1555.
10 R.W. Read, R.J. Spear and W.P. Norris, Aust. J. Chem., 36 (1983) 1227.
11 (a) H.E. Kissinger, Anal. Chem., 29 (1957) 1702.
(b) H.E. Kissinger, J. Res. Natl. Bur. Stand., 57 (1956) 217.
12 R.G. Patel and M.M. Chaudhri, Thermal Decomposition of Tetracene, in Proc. 4th Symp. Chemical Problems Concerned with the Stability of Explosives, Molle, 1976, pp. 347 ff.
13 G. Norwitz, M. Everett and M.T. Gurbarg, Thermochim. Acta, 12 (1975) 227.
14 T. Ozawa, Bull. Chem. Soc. Jpn., 38 (1965) 1881.
15 (a) R.M. Rogers and L.C. Smith, Thermochim. Acta, 1 (1970) 1.
(b) R.M. Rogers and E.D. Morris, Jr., Anal. Chem., 38 (1966) 412.
16 T.B. Tang, Thermochim. Acta, 58 (1982) 373.
17 M.E. Brown and G.M. Swallowe, Thermochim. Acta, 49 (1981) 333.
18 W.E. Garner and H.R. Hailes, Proc. R. Soc. (London), Ser. A, 139 (1933) 576.
19 A.E. Ubbelohde, in W.E. Garner (Ed.), Chemistry of the Solid State, Butterworth, London, 1955, p. 271.
20 Huang Hao Chuan, Proc. 11th Symp. Explosives and Pyrotechnics, Philadelphia, PA, 1981, pap. 13.
21 G. Krien, 3rd Symp. Chemical Problems Connected with the Stability of Explosives, Ystad, 1973, pp. 33 ff.
22 P.G. Fox, J. Solid State Chem., 2 (1970) 491.
23 W.E. Garner, in ref. 18, pp. 232.
24 R.G. Patel and M.M. Chaudhri, Thermochim. Acta, 25 (1978) 247.
25 J. Harris, Thermochim. Acta, 41 (1980) 1.
26 P.P. Elischer and R.J. Spear, Materials Research Laboratories Report, 1984, MRL-R-918.